ORIGINAL ARTICLE

Characterisation, Performance and Optimisation of Nanocellulose Metalworking Fluid (MWF) for Green Machining Process

J. Kananathan[1], M. Samykano[1*], K. Kadirgama[2], A. K. Amirruddin[1], D. Ramasamy[1], and L. Samylingam[3]

[1]College of Engineering, Universiti Malaysia Pahang, 26300 Gambang, Kuantan, Pahang, Malaysia
[2]Faculty of Mechanical & Automotive Engineering Technology, Universiti Malaysia Pahang, 26600 Pekan, Pahang, Malaysia
[3]Research Centre for Nano-Materials and Energy Technology (RCNMET), School of Engineering and Technology, Sunway University, Bandar Sunway, 47500 Selangor, Malaysia

ABSTRACT – The present research attempts to develop a hybrid coolant by mixing alumina nanoparticles with cellulose nanocrystal (CNC) into ethylene glycol-water (60:40) and investigate the viability of formulated hybrid nanocoolant (CNC-Al$_2$O$_3$-EG-Water) towards enhancing the machining behavior. The two-step method has been adapted to develop the hybrid nanocoolant at various volume concentrations (0.1, 0.5, and 0.9%). Results indicated a significant enhancement in thermal properties and tribological behaviour of the developed hybrid coolant. The thermal conductivity improved by 20-25% compared to the metal working fluid (MWF) with thermal conductivity of 0.55 W/m°C. Besides, a reduction in wear and friction coefficient was observed with the escalation in the nanoparticle concentration. The machining performance of the developed hybrid coolant was evaluated using Minimum Quantity Lubrication (MQL) in the turning of mild steel. A regression model was developed to assess the deviations in the tool flank wear and surface roughness in terms of feed, cutting speed, depth of the cut, and nanoparticle concentration using Response Surface Methodology (RSM). The mathematical modeling shows that cutting speed has the most significant impact on surface roughness and tool wear, followed by feed rate. The depth of cut does not affect surface roughness or tool wear. Surface roughness achieved 24% reduction, 39% enhancement in tool length of cut, and 33.33% improvement in tool life span. From this, the surface roughness was primarily affected by spindle cutting speed, feed rate, and then cutting depth while utilising either conventional water or composite nanofluid as a coolant. The developed hybrid coolant manifestly improved the machining behaviour.

INTRODUCTION

Traditional machining plays a substantial role in the production process through the elimination of excess materials in the form of chips to develop shapes with high dimensional precision and surface finish [1, 2]. Cutting fluids, cutting tools, and machine tools are the three critical enablers in machining [3]. A cutting instrument is a tool that expels the extra materials by direct contact, while the machining tool delivers the essential movement within the workpiece and the cutting tool. Meanwhile, cutting fluid empowers heat removal and helps in flushing out the produced chip [4]. Over the past years, a significant increase in machining process demands from the manufacturing industry has been reported, implying that the manufacturers have to expand their production to meet the growing needs while retaining their products' quality [5]. The challenge is to boost productivity while reducing costs [6]. Expanding productivity implies the utilisation of a higher value cutting parameter to speed up the process. However, using a higher value of cutting parameters leads to an increase in cutting temperature and energy. The rise in temperature and energy during machining changes the quality of the surface and the instrument lifespan [7].

Green machining is environmentally friendly and will become a requirement for manufacturing enterprises in the near future. Industries will be obliged to investigate dry machining to comply with environmental and health rules. Dry machining benefits include the following: no pollution of the atmosphere (or water); no residue on the swarf, resulting in lower disposal and cleaning costs; no harm to health; and it is non-irritating to the skin and allergy-free. Additionally, it provides cost savings in machining. The cutting liquid or coolant's or MWF's main objective is to expel the heat produced by friction between the workpiece and the cutting tool, which ultimately decreases the upsurge in temperature of the cutting tool [8]. Besides, cutting fluid also aids in the flushing of the produced chips during the machining process. The reduction in cutting equipment temperature will also decrease cutting power at the tool-work interface and further increase the cutting tool's lifespan [9, 10]. Even though the traditional cooling method can improve the machining procedure's performance, a substantial amount of the machining coolant such as oil-based and synthetic water-based coolant utilised in the process increases the manufacturing cost due to the large quantity used. The large amount used could also endanger the environment and humans [11]. As an alternative to the traditional cooling methods, low-consumption, highly efficient, and clean methods such as minimum quantity lubrication (MQL) and cryogenic cooling have been introduced. MQL is

---

ultimately a green technology, and it is the most efficient, energy-saving, and environmentally friendly lubrication system available [12]. It is expected that the average lubrication consumption can be reduced significantly with the adaption of MQL. The coolant type will also further increase the efficiency of MQL, leading to improved lubrication and decreased environmental pollution [13]. It has been reported that MQL is currently one of the best cooling methods and has drawn immense attention from the research communities [14, 15]. MQL method supplies the cutting liquid in a mist state, delivered directly above the cutting zone interface. Since the low quantity of cutting fluid is utilised in the MQL method, the liquid's heat-carriage capacity and lubricating properties should be at their optimum level. Thus, a cutting fluid possessing high thermal conductivity and lubrication properties is preferred and required for the system [16]. Hybrid nanoparticles are nanoparticles comprised of two or more distinct nanometer-sized components. Hybrid nanofluids are fluids produced using hybrid nanoparticles. Suspending tiny solid particles in energy transmission fluids may substantially increase their thermal conductivity, providing a cost-effective and novel method of dramatically improving their heat transfer properties. Nanofluids were identified as the suitable fluid that could satisfy this requirement [17]. Nanofluids are formulated by dispersing particles of size less than 100 nanometers in a base liquid [18]. There are two main approaches employed in developing nanofluids. The two techniques used are the two-step process and one-step process [19]. The addition of nanoparticles has been reported to improve the thermal properties of nanofluids [20] significantly. Nanofluid has also been categorised as a fluid with superior thermophysical and heat transfer properties [21, 22]. Nanofluid with different non-metallic and metallic nanomaterials demonstrated promising performance as an alternative for traditional MWF with the MQL method. The processing characteristics of nanofluids using the MQL technique were evaluated by Wang, Li [23] for three different workpiece materials. They reported that with Al_2O_3 nanofluid, the grinding ability of the hardened nickel-based alloy improved significantly. The grinding conditions minimised the force ratio (0.38), the real grinding energy (62.20 J/mm³) and increased the surface quality as compared to other grinding settings [23]. Wang, Li [23] concluded that Al_2O_3 nanofluids are ideal lubricants for high strength and tough machining materials. The research on hardened AISI 52100 steel MQL nanofluid (Al_2O_3/water) was carried out by Mao, Zou [24], and Mao, Huang [25]. Both groups of scientists decided to investigate the friction and grinding force by adding nanoparticles of Al_2O_3 into deionised water. Setti, Sinha [26] investigated the efficiency using MQL with Al_2O_3/water nanofluid and CuO/water nanofluid. They reported that compared to CuO nanofluid in both dry and wet conditions, Al_2O_3 nanofluid drastically reduced the friction coefficient. Sharma, Singh [27] prepared nanofluid for machining AISI1040 steel by adding 1 vol. % Al_2O_3 nanoparticles (45 nm size). Their effects on surface roughness, tool wear and cutting force in wet machining have been assessed and reported decreased by 5.27%, 28%, and 25.5%, respectively.

To further enhance the MQL method to reduce the cost and improve the effectiveness [28], nanofluids are prepared with the addition of nanomaterials obtained from natural resources like plants [29]. Cellulose Nanocrystals (CNC) are nano-structured cellulose obtained from various plants, mainly from Canadian Hemlock [30]. The obtained CNC was blended with alumina nanoparticles and ethylene glycol (EG) to formulate a nanofluid-based coolant for machining applications. It is believed that CNC and metal nanoparticles can absorb heat from the cutting tool during machining the workpiece excellently [31]. Due to the high thermal conductivity and optimum viscosity properties, it is believed that CNC-Alumina-based cutting liquid will have a better performance than conventional coolants while prolonging the cutting tool's lifespan and providing a subtle surface finish on the workpiece. The present work aims to investigate the thermophysical properties (stability, thermal conductivity, and viscosity) of hybrid nanofluid for different volume concentrations and evaluate the machining performances compared to metalworking fluid (MWF) coolant in terms of tool wear, surface roughness, wear mechanism, tool life, and chip formation.

MATERIAL AND METHODS

The nanoparticles used in the present work are Cellulose Nanocrystals (CNC) and Aluminium Oxide (Al_2O_3). Both nanoparticles were purchased in powder form from Sigma-Aldrich Chemicals, USA. This nanoparticle has an average particle size of 20-100nm. Several parameters are surmised before blending the CNC with Al_2O_3 nanoparticles. The concentrations of the CNC and Al_2O_3 particles studied are 0.1, 0.5, and 0.9 vol %. The CNC nanoparticles were dispersed in the base liquid containing Al_2O_3 nanoparticles, ethylene glycol, and distilled water (60:40) according to Eq. (1). The volume concentration (φ) in this study is converted to weight concentration (ω) using Eq. (3). The volume of base fluid (60% EG and 40% distilled water) denoted by ΔV is used to dilute the CNC for desired percentage (φ_2) is calculated using Equation (2) with an original condition of V_1 and φ_1.

$$\varphi = \frac{\omega \rho_w}{\left(1 - \frac{\omega}{100}\right)\rho_p + \frac{\omega}{100}\rho_w}, \text{ where } \omega = \left(\frac{m_p}{m_p + m_w}\right) \times 100 \tag{1}$$

$$\Delta V = (V_2 - V_1) = V_1 \left(\frac{\varphi_1}{\varphi_2} - 1\right) \tag{2}$$

$$\varphi = \frac{\frac{M_p}{\rho_p}}{\frac{M_p}{\rho_p} + V_{bf}} \tag{3}$$

where, M_p is the mass of nanoparticles, ρ_p the density of nanoparticles, V_{bf} is the volume of base fluid.

The study comprises two stages. The first stage is preparing a stable composite nanofluid and the assessment, including thermal conductivity and viscosity, of its thermophysical properties. The second stage is an analysis of the prepared nanofluid in machining and assessing the tool's wear, the roughness of the workpiece surface, and the formation of the chip.

Nanofluid Preparation

The technique used to formulate the composite nanofluid is a two-step process. The production of nanofluids involves magnetic stirring and sonication processes. As shown in Figure 1. (a), a magnetic stirrer mixes the nanoparticles for 30 minutes until the CNC and Al_2O_3 powder is completely dispersed into the distilled water and ethylene glycol. The mixing speeds are also set at the appropriate pace to ensure that nanofluids blend not to sprinkled out from the measuring beaker during mixing. After the stirring procedure, the nanofluid is sonicated using an ultrasonic bath as shown in Figure 1. (b) for two hours at 50℃. The sonication procedure improves the stability and dispersion of nanoparticles in the nanofluid.
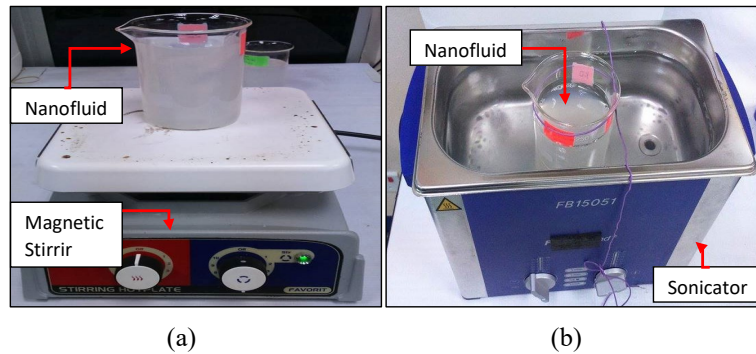

(a) (b)

Figure 1. Nanofluid preparation technique (a) magnetic stirring (b) sonication.

Nanofluid Thermophysical Property Measurement

Stability - sedimentation method

After the sonication procedure, 10ml of nanofluid is filled into a test tube for every volume concentration for the stability observation method. The motivation is to observe the sedimentation process inside the nanofluid and estimate the composite nanofluid's stability.

Measurement of thermal conductivity

Thermal conductivity is one of the domineering properties investigated in this research study. It is calculated to discern the fluid's thermal behaviour through an analyser that relies on the transient hot-wire theory [32]. The KD2 Pro thermal property analyser developed by Decagon Devices, Inc., USA, is used to evaluate thermal conductivity. This thermal analyser quantifies thermal conductivity in the range of 0.200 W/m-K to 2.000 W/m-K with an accuracy of ± 5%. The estimations were executed in controlled temperatures extending from 30 to 70 °C using a Memmert water bath with a precision of 0.1 °C. The validation is performed using the manufacturer's glycerine solution and base liquid 60:40 (EG: Water). The data obtained were compared to data released by the ASHRAE (American Society of Heating, Refrigerating, and Air-conditioning Engineers). The experimental readings are recorded every 15 minutes for 20 readings to prevent experimental inaccuracy after the sample is immersed into the water bath. After completion of a collection of data, the mean value is calculated and used.

Viscosity measurement

Brookfield LVDV-III Rheometer combined with a temperature-regulated bath is used to obtain the composite nanofluids' dynamic viscosity at different nanoparticle percentages. The instrument has an exactness of ±1.0%, and the temperature precision of 0.1 °C ranging from 20 °C to 100 °C. The DV-III Ultra Rheometer works based on a spindle rule located in an adjusted coil with a ULA spindle. The viscosity of the base liquid is measured and compared with values obtained by ASHRAE. In this study, the experiment was performed at the nanofluid temperature of 30 °C, 50 °C, and 70 °C.

Physical Equipment and Material

Workpiece material

Cylindrical mild steel (200mm length and 40mm diameter) bar was used to investigate the machining performances. The chemical composition and physical properties of the workpiece materials used are presented in Table 1 and Table 2.

Table 1. Chemical composition of mild steel (wt.%) [33].

Material	C	Cr	Ni	Si	Mn	P	S	Mo	V
Mild steel	0.15	0.013	< 0.01	0.14	0.79	0.026	0.018	0.004	0.003

Table 2. Properties of mild steel [33].

Physical and chemical properties	Value
Density	7.75 - 8.08 g/cc
Modulus of elasticity	183 - 213 GPa
Tensile strength, ultimate	241 - 2450 MPa
Tensile strength, yield	140 - 2400 MPa
Poissons ratio	0.250 - 0.300
Fatigue strength	758 - 772 MPa
Shear modulus	70.0 - 80.0 GPa
Electrical resistivity	0.0000142 - 0.000142 ohm-cm
Specific heat capacity	0.450 - 0.486 J/g-°C
Thermal conductivity	0.450 - 0.486 J/g-°C
Melting point	25.3 - 93.0 W/m-K

Cutting tool material

An uncoated carbide tool is used as the cutting device in this work. The cutting tool instrument is illustrated in Figure 2. The insert's specifications are rake angle: 10 degrees, inscribed circle: 9.525 mm, insert thickness: 4.7625 mm, nose radius: 7.9502 mm, attached circle: 3.81. The lathe machine used for the turning test is the ERL-1330 lathe machine with a power 2.2Kw motor. The horizontal lathe system is 2000 mm × 965 mm × 190 mm in size, and the maximum speed of the spindle is 2570 rpm.

A metallurgical microscope instrument was used for metallurgical assessment. This microscope is utilised to extricate the wear type and measure the flank wear created on the cutter after the machining test. A low-weight portable surface roughness tester model Mahr Perthometer S2 is used to measure the workpiece's mean roughness depth, R_z, and arithmetic average surface roughness, R_a. Field Emission Scanning Electron Microscope (FESEM) and Energy Dispersive X-ray Spectrometer (EDX) are used to determine all the cutting tools' defects and study the chip pattern after turning the operation. The TM3030Plus examines effective surfaces for compositional data. The Knoop/Vickers Tukon 1202 Hardness Tester was utilised to measure the cutting tool on tool wear. Figure 3 shows the turning process's experimental setup using a lathe machine with metalworking fluid and nanofluids. Surface roughness values are measured by using Pethometer S2. A total of three measurements were taken to determine the average surface roughness of the turning surface. Flank wear is measured using the optical measuring device with the width from the original cutting edge to the limit of wear land. The flank wear measurement is taken after each pass of the machining process (as recommended by ISO 3685:1993, the wear criteria for steel are 0.3 mm).
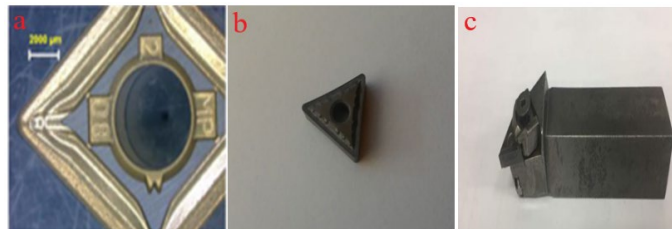

Figure 2. Cutting device (a) rake face of insert (b) cutting tool (c) tool holder.
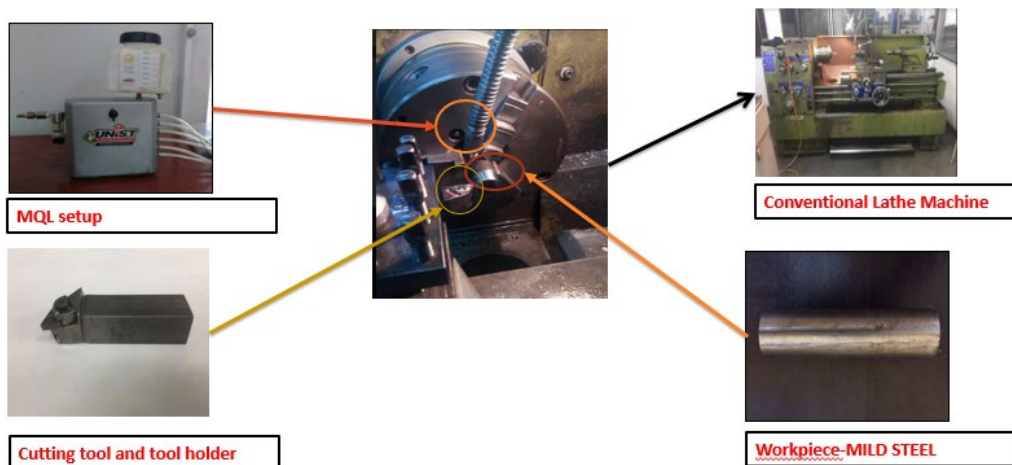

Figure 3. Experimental setup.

Scanning Electron Microscope and Transmission Electron Microscopes

Scanning electron microscope (SEM) is an electron microscope that generates clear micrographs of a sample by scanning the surface with a focused beam of electrons. It is used to determine all the defects on the cutting tool and to study the chip pattern after turning operation. Transmission electron microscopy (TEM) can produce pictures with much greater resolution than a light microscope by utilising electrons as the light source. The fundamental concept is that an electron beam travels through a very thin sample. After interacting with the sample's atoms, some unscathed electrons reach a fluorescent screen, forming a picture. The picture is presented in various shades of grey to indicate the material density in various specimen regions. The picture is enlarged and may be seen immediately on the screen or captured with a camera for post-processing examination. In situ TEM enables the real-time study of nanostructures' microstructural development in response to external active stimuli and their connection to their characteristics.

SEM that was utilised in this study was Hitachi TM3030Plus. This model has a superior SE detector which has been unified in FE-SEM and VP SEM. It can be operated successfully under low vacuum environments and enables fast SE observation without specimen preparation. The Energy Dispersive X-ray Spectrometer (EDX) for the Hitachi TM3030 series comes with the latest silicon drift detector (SDD), large detection area (30 mm^2), and various elemental analyses such as point or area analysis, line scanning, and mapping. The TM3030Plus allows for effective imaging examination with double signals in one image, which is displayed as one collective SE signal provided that the surface has rich information and a BSE signal for compositional data.

Experimental Design and Selection of Cutting Data

The design of experiment (DOE) was utilised to obtain different cutting combinations comprising feed rate, cutting speed, and cutting depth. Additionally, the response surface method (RSM) was used to find the expected response from the combination of the different feed rates, cutting speeds, and cutting depth from the experimental value measured from tool wear and surface roughness, followed by a mathematical model development from the responses. There are essentially two main types of DOEs, Box-Behnken design (BBD) and central composite design (CCD). In this analysis, the Box-Behnken design was considered to evaluate first-order and second-order terms effectively. Besides that, it is cost-effective to operate compared with CCD with the exact number of factors.

Cutting speed, feed rate, and axial depth were the three factors that influence and should be considered in the analysis to explore their impact on surface roughness and tool wear. The designed variables and levels to be employed for the experiments are shown in Table 3. Table 4 shows the total of 15 experimental runs carried out in this study. Factor levels are coded as -1(low level) and +1(high level). The performance of the experimental design was analysed with Minitab 17 statistical software. The result was estimated using ANOVA with a 95% confidence level based on the p-value.

Table 3. Selected parameter input for DOE.

Parameter/ Coding level	-1	1
Cutting speed (rpm)	425	990
Feed rate (mm/rev)	0.05	0.18
Axial depth (mm)	0.5	1.5

Table 4: A 2^3 Factorial design matrixes generated from Minitab 17.

Experiment	Cutting speed (rpm)	Feed rate (mm/rev)	Depth of cut (mm)
1	425	0.1	1.5
2	707	0.18	0.5
3	425	0.1	1.2
4	425	0.18	1.2
5	707	0.05	1.5
6	707	0.05	0.5
7	425	0.05	1.2
8	707	0.1	1.2
9	990	0.1	1.2
10	425	0.1	0.5
11	990	0.05	1.2
12	990	0.1	0.5
13	707	0.18	1.5
14	990	0.18	1.2
15	990	0.1	1.5

RESULTS AND DISCUSSION

Sedimentation Observation - Qualitative Method

The common suspended particles' problems are agglomeration and fast settlement of particles in a fluid [35]. Thus, high durability and enhanced suspension stability are required for optimum heat transfer enhancement. Although no surfactants were used during the preparation of nanofluids, the solution was found to be stable without any sedimentation

observed for up to one month, as shown in Figure 4. Based on the qualitative method (sedimentation observation) used for examining the nanofluid's stability, it is noticed that the ethylene glycol-distilled water with CNC-based nanofluid has achieved good stability for a month. Ramachandran, Hussein [36] also found similar findings. They find that the ultrasonic process prolongs the stability of the nanofluid for up to 3 months. More in-depth investigations have been performed by Maheshwary and Nemade [37] using ZrO_2/H_2O nanofluid to study the sedimentation observation. Their findings showed only a small amount of sedimentation occurs for all base fluid due to the gravitational forces after more than one month of observation. Sundar, Singh [38], in their study, observed that Fe_3O_4 nanoparticles dispersed in a water-ethylene glycol mixture is stable for up to one month. Sarafraz and Hormozi [39] stated that due to the powerful van der Waals interaction, sedimentation of nanofluids occurs. The particles accumulate due to high surface activity as time elapses [40].
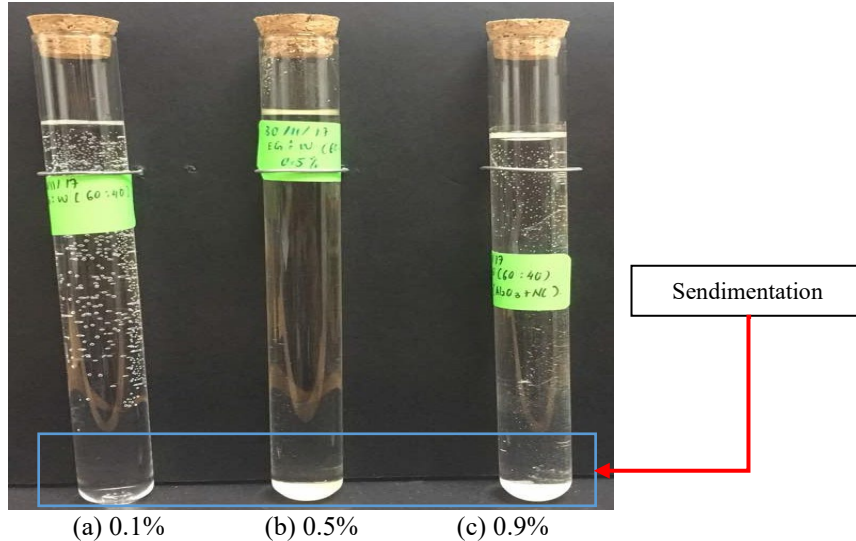

| (a) 0.1% | (b) 0.5% | (c) 0.9% |

Figure 4. Nanofluid Al_2O_3/CNC samples at different concentrations.

UV-Vis Spectrophotometer Evaluation - Quantitative Method

The UV-Vis spectrometer analysis was performed to investigate the structural, optical properties, and solution's stability [42]. The absorbance is monitored and recorded every week to observe the three different prepared composite (Al_2O_3/CNC) nanofluid solutions stability. The data plotted in Figure 5 clearly shows that the three different concentrations' absorbance has reached its stability within the 4-5 days after preparing the solution. From the investigated three concentrations, the 0.1% volume concentration achieved stability first, followed by 0.5%, and finally 0.9%. Furthermore, the stability of the samples over a month of observation was also seen to be stable. Habibzadeh, Kazemi-Beydokhti [41] also reported a similar stability state.
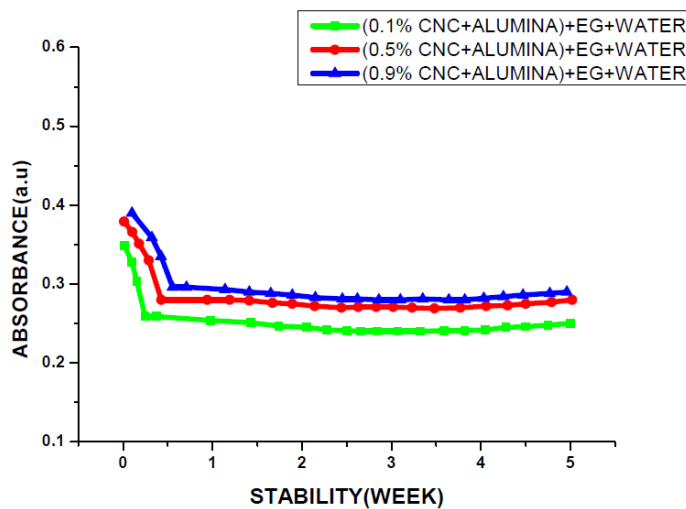

Figure 5. UV-Vis spectrophotometer analysis for different concentrations for one month.

Figure 5 shows the supernatant particle absorbance against the sedimentation graph for the studied three concentrations. It can be clearly seen that Al_2O_3/CNC hybrid nanofluids have been stable for more than a month. After a month, the absorbance was recorded within the range of 0.24 a.u to 0.31 a.u values, indicating that over 70% of these nanofluids' relative concentration was maintained as initial. This pattern illustrates suspended nanofluids' behaviour that

increases with the concentration volume [43]. The colloidal nanofluid's stability is therefore preserved at the specific concentration volume. From this observation, it can be inferred that a lower concentration of nanofluids has the potential for faster sedimentation [44].

Transmission Electron Microscopy

A common method for acquiring an Al_2O_3 and CNC image at high magnification is by using transmission electron microscopy (TEM). The CNC and Al_2O_3 nanoparticles can be clearly seen in Figures 6(a) and 6(b). Meanwhile, Figure 6(c) shows the image of blended Al_2O_3/CNC. A good blending has been observed, which was anticipated for further studies.
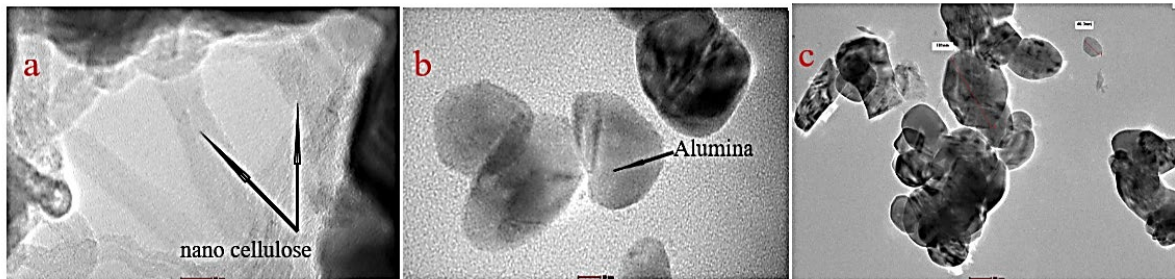

Figure 6. TEM images of (a) CNC, (b) Al_2O_3, and (c) Al_2O_3/CNC.

FESEM Observation

The morphological and size characteristics of the prepared hybrid nanoparticles were analysed using FESEM. As illustrated in Figure 7, nanoparticles were found to be circular with a mean dimension of 13 nm. Hatami and Okhovati [45] observed round-shaped nanoparticles in a similar study but with dissimilar sizes. In a study conducted by Meriläinen, Seppälä [46], it was reported that small and circular shape particles significantly enhance the nanofluids' heat transfer properties while maintaining the pressure effect.
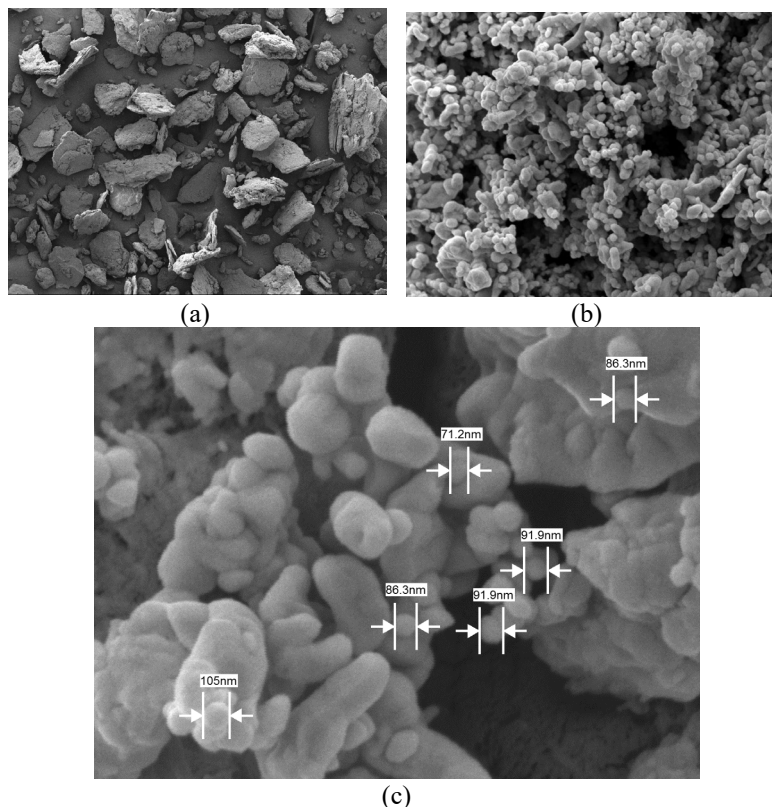

(a)

(b)

(c)

Figure 7. FESEM image of Al_2O_3/CNC nanoparticles (a) 15k, (b) 100 and (c) 50k magnification.

Thermophysical Properties Evaluation of Nanofluid

Thermal conductivity

The thermal conductivity measurement was carried out at three different temperatures (30 °C, 50 °C, and 70 °C) for each volume concentration. The measurement was also performed for conventional machining coolant, MWF. Figure 8 shows the thermal conductivity reading of conventional machining coolant (MWF) and the nanofluid of various volume

concentrations. Enhancement in thermal conductivity can be observed as the temperature and volume concentration increase. Similar results were also obtained by Chiam, Azmi [47] in their work examining the thermal conductivity for Al_2O_3 dispersed in water and EG.
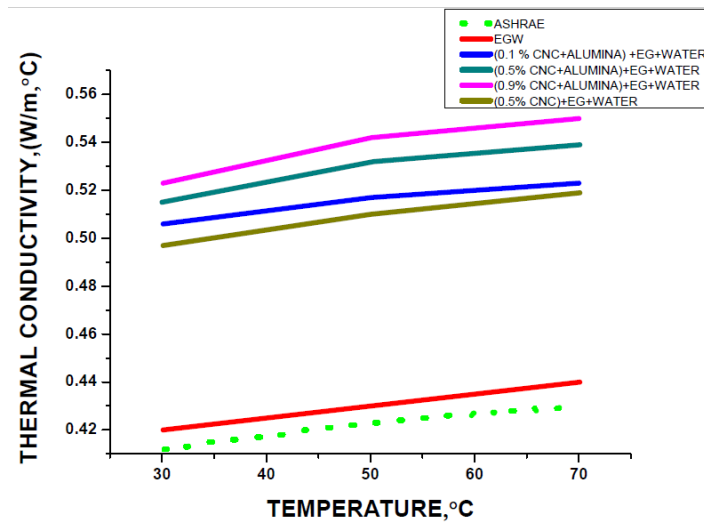

Figure 8. Thermal conductivity with respect to temperature

The thermal conductivity results of Al_2O_3/CNC nanofluids with volume concentrations of 0.1 %, 0.5 %, and 0.9 % have been demonstrated in Figure 8. The thermal conductivity is seen to increase when the nanoparticle concentration increases in the nanofluids. In a study conducted by Acevedo-Fani, Salvia-Trujillo [48], the authors stated that the collision between particles escalates as the concentration increases. Vajjha and Das [49] reported the impact of the concentration of nanoparticles toward improving thermal conductance.

Based on Figure 9, the composite nanofluid containing Al_2O_3/CNC shows a better thermal property in comparison to CNC incorporated nanofluids. This is because Al_2O_3 has better thermal properties than other nanoparticles. Meanwhile, high collisions of particles lead to high kinetic energy [50]. Hence, the prepared composite nanofluid has higher thermal conductivity than CNC incorporated nanofluid. The presence of higher kinetic energy at high temperatures increases heat transfer rate as the particles can transfer heat directly from one to another at high temperatures [51]. Besides, it was observed that as the concentration of Al_2O_3 in the composite Al_2O_3/CNC incorporated nanofluid increases, the value of thermal conductivity increases as well. As shown in Figure 9, the composite nanofluid thermal conductivity value is greater than that of traditional coolant machining. It thus indicates that the tendency of the composite nanofluid containing nanocellulose to absorb heat produced during the machining operation is exceptionally high at the heat generation interface between the workpiece and the cutting tool. Nanofluid's high thermal conductivity properties help remove most of the heat produced [52].
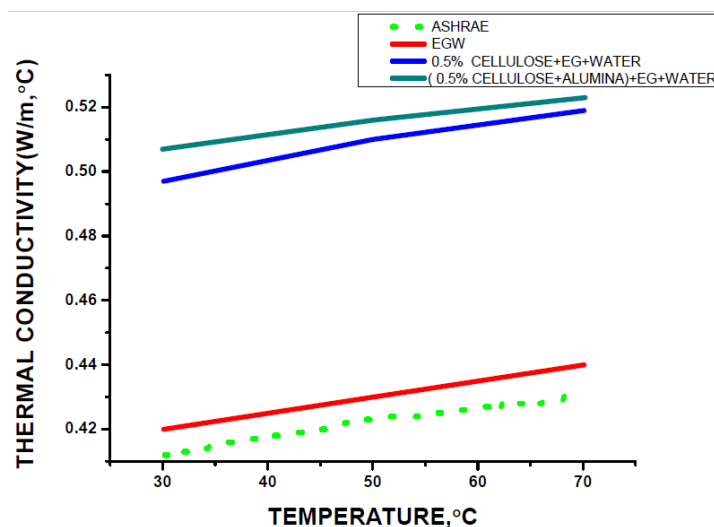

Figure 9. Composite nanofluid and single nanocelulose coolant thermal conductivity measurement with respect to temperature.

Effect on nanoparticles concentration on thermal conductivity

A linear relationship is seen between the concentration of nanoparticles in nanofluid and the thermal conductivity. The thermal conductivity of Al_2O_3/CNC hybrid nanofluid increases from 0.515 to 0.541 W/m K under the same

temperature as volume fraction increased. In the study by Hamid and Aiyelaagbe [53], it was reported that improvement in thermal conductivity of Al_2O_3/CNC water and ethylene glycol composite nanofluid was 13.8 % of every 1 % concentration and 22.1 % in 3 % concentration at the constant temperature. In another study conducted by Nabi, De Vriend [54], the enhancement was reported in thermal conductivity from 22.8 % out of 3 % concentration. In this study, an excellent improvement in thermal conductivity with a value of 150 % was accomplished at a 1.5 % volume fraction of (Al_2O_3/CNC) composite particles.

Temperature effect on thermal conductivity

At high temperatures, the Brownian motion of particles upsurges due to the high kinetic energy thus enhanced the thermal conductivity. The temperature increase is seen to improve the thermal conductivity of nanofluids. When the temperature raised from 30 ºC to 70 ºC, the composite nanofluid (Al_2O_3/CNC) thermal conductivity improved from 0.515 to 0.539 W/m K in 2 % volume concentration. However, high temperature in nanofluids leads to the agglomeration of nanoparticles and reduction of repulsive forces between them. This results in a reduction of thermal conductivity and stability of nanofluids. In a study by Farbod and Ahangarpour [55], it was reported that by increasing the temperature to 40 ºC, the thermal conductivity of Ag-MWCNTs incorporated composite nanofluid was improved. However, the value of thermal conductivity decreased by further increasing the temperature (above 40 ºC). In another study conducted by Esfahani, Zhang [56], it was indicated that the influence of dispersant could be prevented by increasing the temperature from 60 ℃ to 65 ºC, leading to unsuspended nanoparticles and reduced thermal conductivity.

Dynamic Viscosity of Nanofluids

The viscosity measurement was initially taken with the base fluid to verify the correct steps and obtain accurate data. Previous studies that have been used as a benchmark are from Kulkarni, Crespo [57], and Vajjha, Das [58]. The measurements were then carried out after verification of the accuracy of the instruments. According to Vajjha, Das [58], the water and ethylene glycol mixture shows Newtonian behaviour. Based on Figure 10, it is observed that, as the volume concentration increases, the viscosity of nanofluid increases. This is in line with the fact that the fluid internal shear stress increases by increasing the nanoparticle concentration suspended in the base fluid, and therefore viscosity also increases [59]. This exhibits a more complicated behaviour and has a different relationship than simple linearity between shear stress and velocity gradient, following Non-Newtonian fluid behaviour. Previous literature such as Namburu, Kulkarni [60], and Fedele, Colla [61] found a similar effect of volume concentration on the viscosity. Figure 10 proves that as the temperature increase, the viscosity decreases. Li, Guo [62] elaborated that based on a molecular perspective, the temperature effect on nanofluid viscosity can be verified. They assert that the intermolecular gap becomes more significant as the temperature rises, leading to a decreased viscosity pattern.
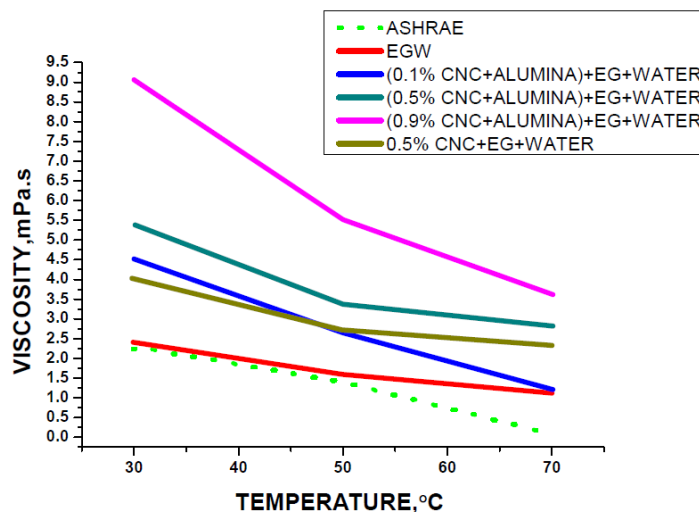

Figure 10. Viscosity with respect to temperature.

Selection of Nanofluid

A coolant should exhibit lower viscosity and good thermal conductivity for optimum behaviour. Thus, nanofluids should meet or exceed those criteria to be considered a suitable replacement for conventional coolants. As shown in Figure 11(a), the present findings indicate that the investigated nanofluid containing CNC+Alumina exhibited a higher thermal conductivity than the conventional machining coolant. Figure 11(b) shows the residual plot for Ra RSM: MWF. A high viscous coolant will cause uneven material removal on the workpiece during metal cutting and require high pumping power to spray the coolant; thus, a major modification is required in the machining [63]. Considering both the thermal properties, the 0.5 % concentrated nanofluid was identified as suitable for performance investigation as it has low viscosity and high thermal conductivity value to avoid all major constraints. Therefore, 0.5% nanofluid volume concentration is used for turning operation to determine its machining performance relative to conventional metalworking fluid (MWF).
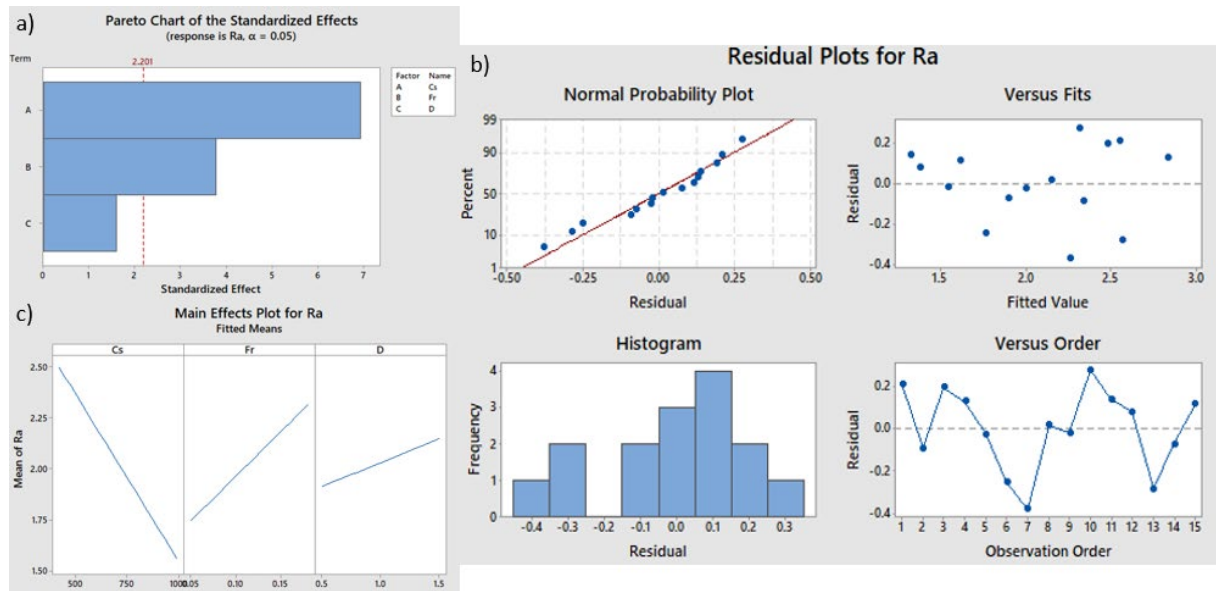
Figure 11. (a) Pareto chart plotted for Ra, (b) residual plot for Ra and (c) main effect plot for Ra using RSM: MWF.

Response Model

The linear model shows the relationship between the turning responses and independent variables represented as the following expression Eq. (4) and Eq. (5).

$$y' = (cutting\ speed) + (Feed\ rate) + (Depth\ of\ cut) + D \qquad (4)$$

Where a, b, c, and D are the constants. Eq. (4) can be stated in the following form:

$$y'' = \beta_0 x_0 + \beta_1 x_1 + \beta_2 x_2 + \beta_3 x_3 \qquad (5)$$

Where y = turning response, x_0 = 1(variable), x_1 = cutting speed, x_2 = feed rate, x_3 = cutting depth. β_0, β_1, β_2 and β_3 are the model parameter.

Development of linear surface roughness model: MWF and hybrid nanofluid

After the first pass of the turning experiment, set for 20 mm of cutting, the surface roughness reading result is used to produce a linear Eq. (5) model. To calculate this parameter, the response surface method is used with the aid of Minitab 17 Software. Linear equations used to predict the turning experiment's surface roughness performed with metalworking fluid coolant and composite nanocellulose alumina-based coolant is expressed in Eq. (6) and Eq. (7).

Surface roughness using MWF coolant is:

$$Ra = 2.465 - 0.001654\ Cs + 4.37\ Fr + 0.234\ D \qquad (6)$$

Surface roughness using hybrid nanocoolant is:

$$Ra = 2.057 - 0.001682\ Cs + 4.80\ Fr + 0.308\ D \qquad (7)$$

From the ANOVA analysis for surface roughness using a conventional coolant and composite nanocoolant, the p-value was found to be less than 0.05, suggesting the importance of the independent variables (Table 5). According to the Pareto chart in Figure 11(a), in which the bar length is proportional to the absolute values of the estimated effect with a 95% confidence level, it is verified that cutting speed demonstrates the most significant effect on the surface roughness for both the conventional coolant and composite nanocoolant, as in Figure 12(c) — followed by the feed rate that almost half of the cutting speed effect. The depth contribution to the surface roughness was not significant as its effect is below the standardised effect of 2.201. The normal probability plot in Figure 12(a) shows that the point is aligned along the best-fit line. It can be said that the results obtained from the experiment fit and satisfy the mathematical model. Figure 12(b) shows the residual plot for Ra using RSM for hybrid nanocoolant. Comparing the ANOVA result for both the conventional and composite nanocoolant as in Figure 12(a) indicates that the cutting speed contribution to the surface roughness has been reduced when using the composite nanocoolant over conventional coolant. Table 6 represents the analysis of ANOVA for Ra using hybrid nanocoolant.

Table 5. ANOVA analysis for Ra using MWF.

Source	Sum of squares	Contribution	df	Mean square	F-value	p-value
Model	3.04	85.55	3	1.01	21.71	<0.0001
Cutting speed	2.25	63.50	1	2.25	48.18	<0.0001
Feed rate	0.66	18.73	1	0.66	14.22	0.0031
Depth	0.12	3.33	1	0.12	2.53	0.134
Error/Residue	0.51		11	0.047		
Total	3.55		14			
S = 0.22, PRESS = 0.986 R-Sq = 85.55 %, R-Sq(adj) = 81.61 %, R-Sq(pred) = 72.18 %						

From the main effect plots Figure 11(c), it can be observed that to obtain a lesser worn out and increased tool life, the suggested cutting parameter is by reducing the cutting speed and raising the feed rate, which is also supported by the findings in Figure 12(c).

Table 6. Analysis of ANOVA for Ra using hybrid nanocoolant.

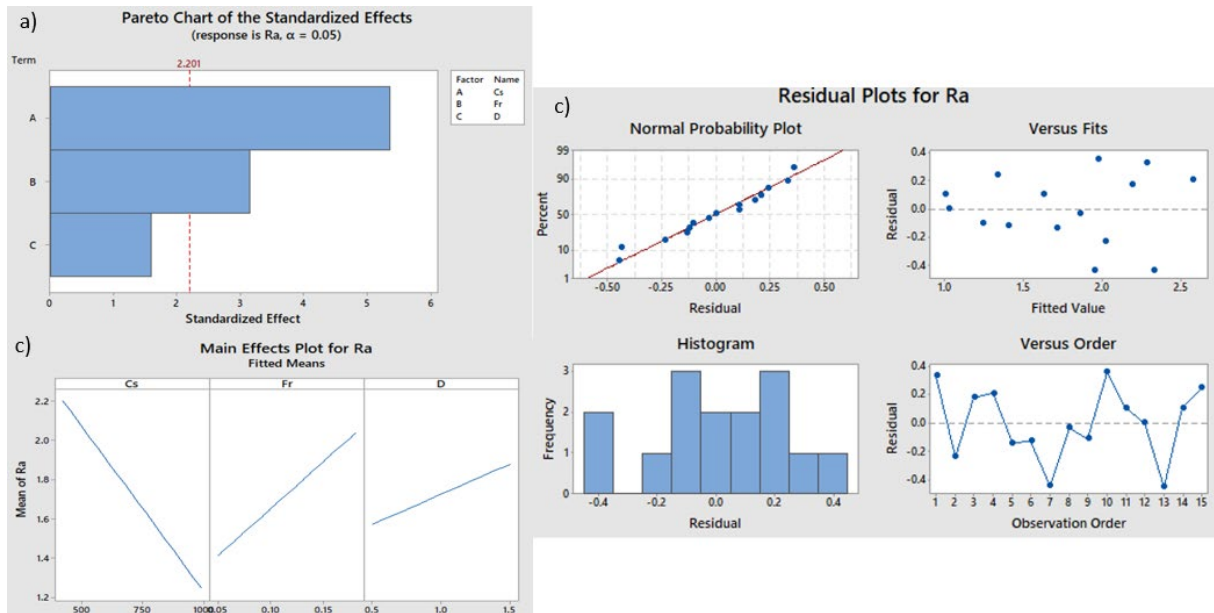| Source	Sum of squares	Contribution (%)	df	Mean square	F-value	p-value
Model	3.33	78.96	3	1.11	13.76	<0.0001
Cutting speed	2.32	55.14	1	2.32	28.77	<0.0001
Feed rate	0.80	18.99	1	0.80	9.90	0.009
Depth	0.20	4.82	1	0.20	2.52	0.141
Residual	0.89		11	0.081		
Total	4.22		14			
S = 0.28, PRESS = 1.72, R-Sq(adj) = 73.22 %, R-Sq(pred) = 59.33 %						

Figure 12. (a) Pareto chart plotted for Ra, (b) residual plot for Ra, and (c) main effect plot for Ra using RSM for hybrid nanocoolant.

Analysis comparison on the experimental and mathematical model using MWF and hybrid nanocoolant for surface roughness

After turning 20 mm for every 15 sets of metalworking fluid parameters (water coolant and composite nanofluid coolant), the mild steel surfaces' roughness was measured three times at different steel surfaces to calculate the average value of the surface roughness, Ra.
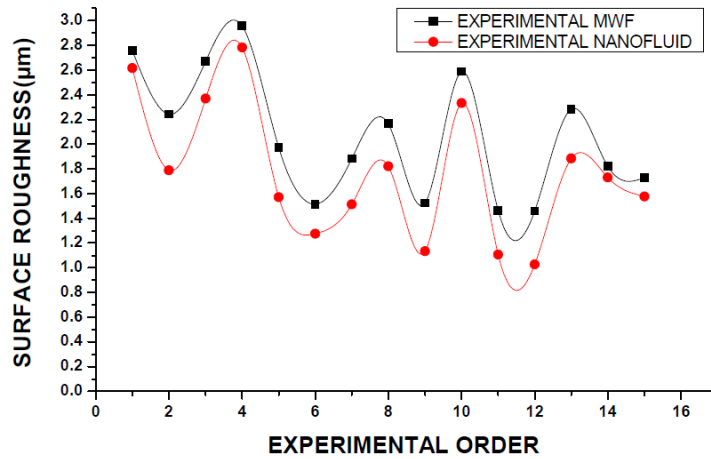
Figure 13: Comparison of machining results for Ra using MWF and hybrid nanocoolant.

Based on the graph in Figure 13, it can be noticed that the average value of surface roughness, Ra for machining using composite nanofluid, has produced finer surface roughness compared to machining using water coolant. The differences significantly could be observed from the graph that machining using water coolant produce a rougher surface. It can be concluded that Ra decreases on the increasing of cutting speed. Hence it produced a better quality of the surface. On the other hand, the surface roughness tends to decrease with the escalation in cutting speed at a constant feed rate [64]. Lower surface roughness values or high-quality surface finish on the machined workpiece can be assumed due to lower cutting force and less heat lost to the workpiece during the machining process at higher cutting speeds during machining procedures [65].

Kumar, Singh [66] has stated that when the cutting speed is increased, the period of the chip stays in contact with the tool decreases, and the heat generated is removed and carried away by the chip. Moreover, when lubricants are used in flood conditions, a large quantity of coolant may not have reached the cutting zone and causing heat accumulation at the cutting area. In the MQL system, the cutting fluid is supplied at high pressure and high velocity directly to the interface of the cutting tool and chip that reduces friction force and increases tool life, leading to a better quality surface finish the workpiece [67]. The feed rate also influences the surface consistency. The experiment has shown that as the feed rate increases, surface roughness increases. This is because the heat produced in the cutting region increases as the feed rate increases due to the high material removal rate during the machining process [68]. Hence, it will increase tool wear, which reduces the sharpness of the flank face of the cutting tool, which will affect the surface roughness of the workpiece upon machining [69]. ANOVA results have also revealed that the cutting speed and feed rate are significant factors affecting the quality of product surface. Therefore, the surface quality can be improved by decreasing the feed rate.

Adapting the MQL system, nanofluids are sprayed out like fog from the nozzle under the impression of high-pressure gas. Through precipitation or adsorption, the high polarity nanoparticles can bind to the tool-workpiece interface forming a layered film [70]. Nanoparticles in the layer film help to relieve the high pressure, thereby reducing the sliding machining force. It acts as a coolant lubricant to decrease the friction of the instrument and workpiece interface rather than to decrease the high heat generation in the cutting field [71].

Development of linear tool wear model with MWF and hybrid nanocoolant

Linear equations are used to predict the tool wear of the turning experiment performed with MWF, and hybrid nanocoolant is expressed as Eq (8) and Eq (9). To calculate this parameter, the response surface method is used with the aid of Minitab 17 Software.

$$Tool\ wear\ MWF\ =0.3172+0.000049\ Cs-0.1609\ Fr+0.0096\ D \tag{8}$$

$$Tool\ wear\ hybrid\ nanocoolant =0.323-0.000049\ Cs+0.063\ Fr+0.0138\ D \tag{9}$$

From the ANOVA analysis for tool wears using a conventional coolant and composite nanocoolant, the p-value of the main effects is smaller than 0.05 implies the significance of the independent factors for the conventional coolant. However, the p-value is more than 0.05 for the composite nanocoolant (in Table 7). According to the Pareto chart in Figure 14(a), the bar length is proportional to the absolute values of the estimated effect with a 95 % confidence level; thus, it is affirmed that cutting speed demonstrates the most significant effect on the tool wear for conventional coolant. However, when using composite nanocoolant (Figure 15(a)), no significant effect on the tool is wear caused by the cutting speed, feed rate, and depth of cut is observed. The three parameters show no significance as their effect is below the standardised effect of 2.201. The normal probability plot Figure 14(b) shows that the point is aligned along the best-fit line. It can be said that results obtained from the experiment fit and satisfy the mathematical model obtained. Comparing the ANOVA in Table 8, results for both conventional and composite nanocoolant show that the cutting speed and feed rate do not contribute to the tool wear when using the composite nanocoolant over conventional coolant. It can be said that the composite coolant helps (in Figure 15(b)) in reducing the high-temperature generation at the tool-work interface

by providing high cooling during the high-speed cutting. The temperature generation during high-speed cutting has been reduced significantly; thus, no significant effect on the cutting speed. This increased cooling has reduced the high-temperature build-up at the cutting tool and promoted an enhanced cutting tool life [72]. From the main effect plots in Figure 14(c), it can be observed that to obtain a lesser warn out and increased tool life, the suggested cutting parameter is by increasing the cutting speed with reduced feed rate using the composite nanofluid. The findings from Figure 15(c) further support this conclusion. However, for lesser tools warn out using conventional coolant, the machining parameter is suggested to have lower cutting speed and increased feed rate.

Table 7. Analysis of ANOVA for tool wear using MWF.

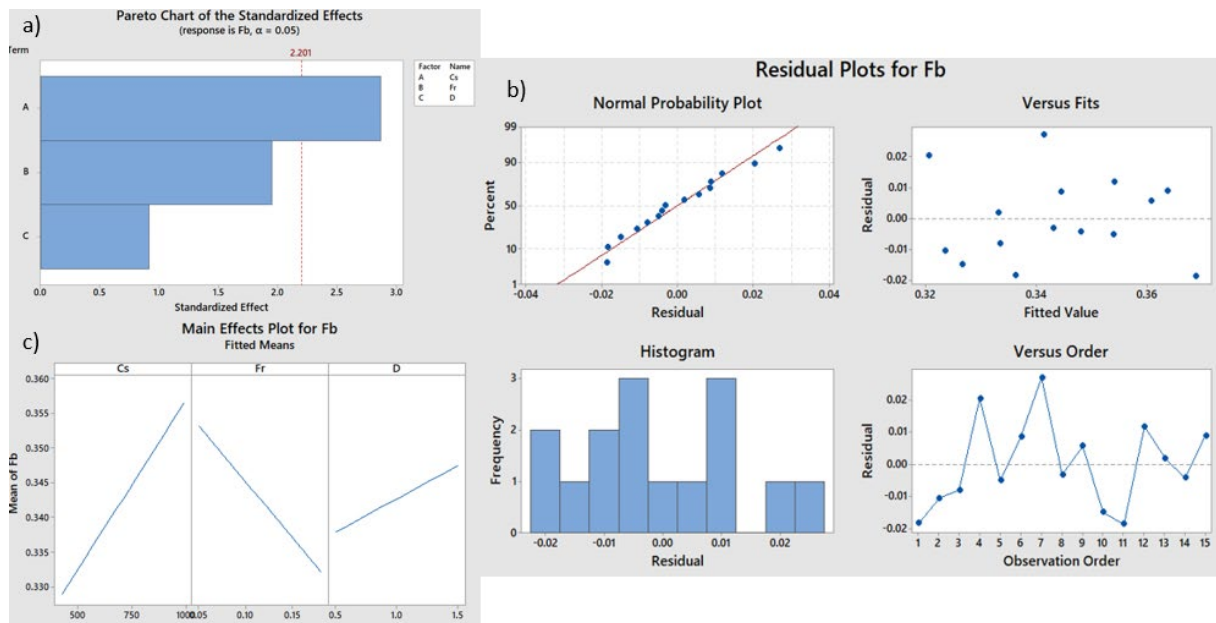| Source	Sum of squares	Contribution	df	Mean square	F-value	p-value
Model	3.078E-003	54.33	3	0.001026	4.36	0.03
Cutting speed	1.987E-3	35.07	1	0.001940	8.25	0.015
Feed rate	8.94E-4	15.79	1	0.000897	3.81	0.077
Depth	1.97E-4	3.47	1	0.000197	0.84	0.380
Error/Residue	2.58E-3		11	0.000235		
Total	5.66E-3		14			
S = 0.0153, PRESS = 0.0049902, R-Sq = 54.33 %, R-Sq(adj) = 41.87 %, R-Sq(pred) = 11.92 %						

Figure 14. (a) Pareto chart plotted for tool wear, (b) residual plot for tool wear, and (c) main effect plot for tool wear using RSM: MWF.

Table 8. Analysis of ANOVA for tool wear using hybrid nanocoolant.

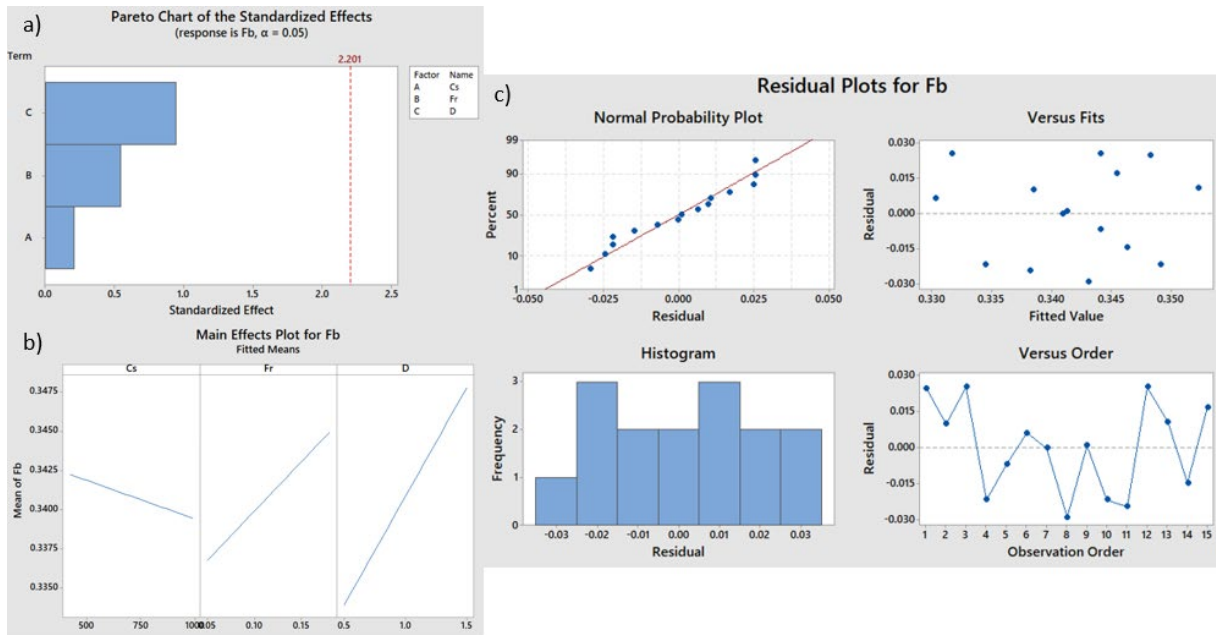| Source	Sum of squares	Contribution	df	Mean square	F-value	p-value
Model	5.66E-004	10	3	1.89E-04	0.41	0.750
Cutting speed	1.8E-005	0.32	1	2E-05	0.04	0.840
Feed rate	1.37E-004	2.43	1	1.36E-04	0.29	0.598
Depth	5.08E-003	7.27	1	4.1E-04	0.89	0.366
Error/Residue	5.6E-004		11	4.62E-.4		
Total	5.051E+005		14			
S = 0.02149, PRESS = 0.0049902, R-Sq =10 %, R-Sq(adj) = 0 %						

Figure 15. (a) Pareto chart plotted for tool wear, (b) residual plot for tool wear, and (c) main effect plot for tool wear using RSM: hybrid nanocoolant.

Analysis comparison on the experimental and mathematical model of tool length of cut using: MWF and hybrid nanocoolant

Figure 16 shows the comparison of the cutting tool length of cut before it reaches the wear criterion of the experimental and predicted model using MWF and composite nanofluid. It shows that the predicted values satisfied the experimental findings with less than 10% of error. This validates the experimental work performed. Figure 17(a) and Figure 17(b) show the progression in flank wear distance with machining distance in turning cylindrical mild steel using water coolant and composite nanofluid. The mild steel workpiece of 20 mm in length will be cut by the cutting tool for each pass. The flank wear is assessed after each move, and the turning operation will be continued until the wear criterion is met according to ISO 3865:1977 (the flank wears $\geq$ 0.3 mm). It is also observed from Figure 17(a) that cutting parameter No. 9 (cutting speed = 990 rpm, feed rate = 0.1 mm/rev, and cutting depth = 1.2 mm) has the highest flank wear rate compared to other cutting parameters in the metalworking fluid coolant experiment. Flank wear meets the tool wear criterion with a total cutting length of around 45 mm for cutting parameter No. 1. Meanwhile, for cutting parameter No. 4 (cutting speed 425 rpm, feed rate 0.18 mm/rev, and cutting depth = 1.2 mm), the cutting tool has achieved wear criteria at a total cutting length of around 88 mm. This postulates the effect on flank wear of cutting speed and feed rate. Increased cutting speed and decreased feed rate increases flank wear, resulting in quicker tool wear [69]. These findings were further proved with the mathematical model analysis using surface response methodology, showing a similar trend from the main effect plots. According to Altin, Nalbant [73], the formation of flank wear on the cutting tool is affected by high heat generation at a higher cutting speed during the metal cutting process. Thus, the tool's cutting edge is softened at high temperatures during the metal cutting process at the tool-chip interphase, which gradually causes gradual wear to occur [74].
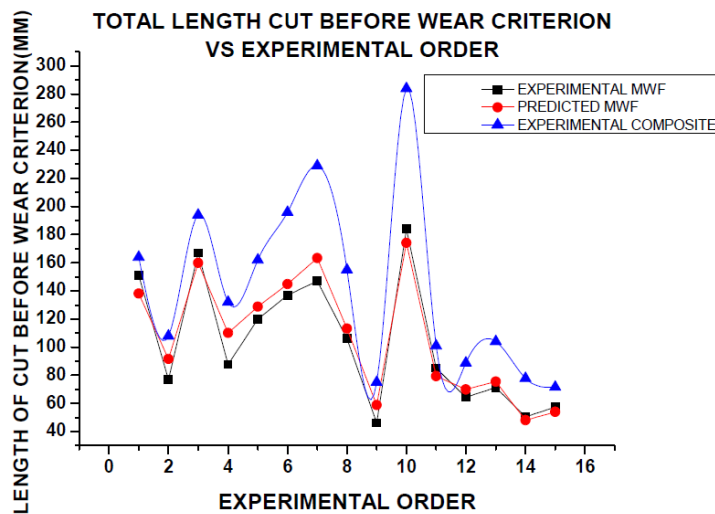

Figure 16. Machining result for tool wear using water coolant and composite nanocoolant with the mathematical model prediction.

However, using the composite (nanocellulose+alumina) nanocoolant, the total length of cut was found to increase during the turning operation of mild steel workpiece at similar cutting parameters, as shown in Figure 17(b). Cutting parameters No. 9 and No. 4 significantly increase the overall cut duration to meet the wear criterion of ISO 3865:1977 under the same cutting conditions. For cutting parameters No. 9 and No. 4, respectively, flank wear meets the wear criterion of about 78 mm and 135 mm of the total cut length. Therefore, the composite has a significant flank wear rate enchantment. A similar result was also obtained by Vasu and Pradeep Kumar Reddy [75] on prolonged tool failure using nanofluid as a coolant. The superior nanofluid properties allow the hardness of the cutting tool to be maintained, and the time is extended to meet the wear criterion for failure.
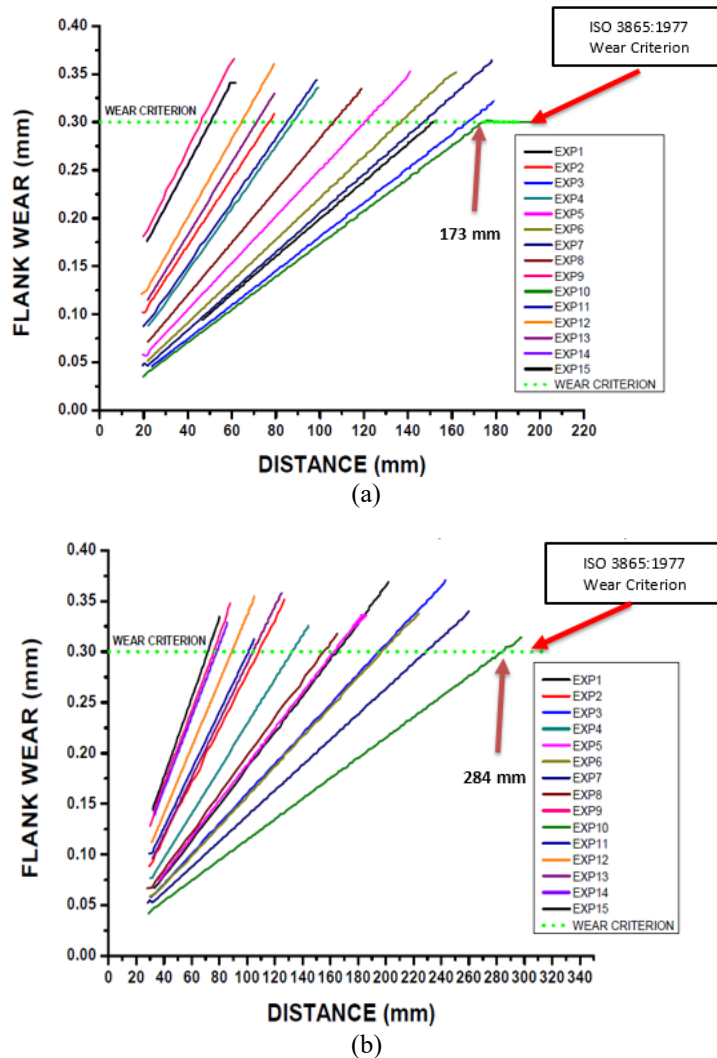

(a)

(b)

Figure 17. Progression of flank wear by distance for turning with (a) MWF (b) composite nanocoolant.

Analysis of chip formation on turning operation using MWF and hybrid nanocoolant

The unwanted metal is removed during the turning process in the form of chips. The chip helps to remove the heat produced during the turning. Nonetheless, the pattern of the chip generated affects the processing results. As the cutting speed is increased, the output heat is also increased [76]. Therefore, the chip produced will be continuous, and the friction forces between the chip and the cutting tool will gradually increase [77]. This is because, as shown in Figure 18, the continuous chip would continuously move over the rake face of the cutting tool. The greater the impact of friction, the higher the heat produced by the cutting tool. Figure 18(a) shows the chip formation progression when using MWF coolant, and Figure 18(b) shows the discontinuous chip formed during turning operation using ethylene glycol/nano cellulose+ alumina-based nanofluid coolant. The enhanced higher thermal conductivity properties of composite nanofluid promote high heat transfer during machining, thus less heat generation at the tool-work interface along with reduced friction at the tool-chip interface providing better chip formation during turning operation [77].

During machining at high cutting speed, it can be seen that it leads to thinner chips' production. This is observed with the use of conventional coolant. The arc chip size gets longer without breaking due to the high heat generated from greater friction and cutting force, thus causing a continuous chip [78]. Conventional coolant does not effectively caries away heat generated due to the high cutting speed. Figure 19(b) demonstrates the chip created during the machining with the MQL system utilising composite nanofluid coolant. The arc chip size gets smaller resulting in discontinuous chip formation.

This proves that the hybrid coolant's superior thermophysical properties can carry away heat generated and provide lubricity, resulting in less peeling off the cutting tool and longer tool life.
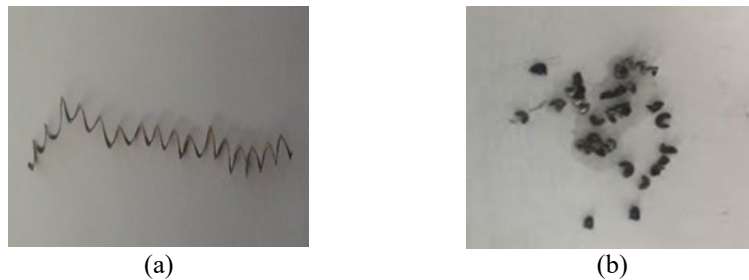

(a) (b)

Figure 18. The chip formation of MQL system (a) MWF (b) composite nanocoolant.

Analysis of tool failure on turning performance using MWF and hybrid nanocoolant

A 20 mm cut length for the first pass for every experimental set is done to measure the tool life. The flank wear or major fracture obtained on the cutting tool will be measured using an optical microscope connected to a camera and computer. If the flank wear obtained did not reach 0.3mm, the experiment will be repeated with 20 mm length of the cut, and the tool wear measurement is repeated. This step is repeated until the flank wear reaches the range of about 0.3 mm to 0.35 mm. Every 20 mm pass, the time is recorded, and the total time taken to reach its wear criterion is tabulated. Table 9 shows the relationship between flank wear and the cutting instrument's total time to achieve tool wear criteria.

Table 9. Relationship between flank wear and total time taken to reach the flank wear criteria using MWF and hybrid nanocoolant.

| Experiment | Coolant type | | | |
| | Metal working fluid (MWF) | | Hybrid nanofluid | |
	Flank wear (mm)	Total time taken (s)	Flank wear(mm)	Total time taken (s)
1	0.3178	198	0.3729	254
2	0.3128	32	0.3482	53
3	0.3252	226	0.3694	311
4	0.3407	63	0.3273	94
5	0.3488	230	0.3371	307
6	0.3528	269	0.3364	384
7	0.3681	452	0.3407	678
8	0.3397	96	0.3139	134
9	0.3663	24	0.3421	36
10	0.3116	226	0.3126	395
11	0.3502	97	0.3136	97
12	0.3657	36	0.3568	48
13	0.3348	32	0.3629	53
14	0.3436	13	0.3316	20
15	0.3724	24	0.3621	36

It is noted that the cutting tool achieves the ISO wear criterion faster under the MWF turning operation than the cutting tool under the nanofluid turning operation. This is because the enhanced viscosity properties of hybrid nanofluid providing good lubricity during machining reduced the friction at the tool-chip interface. Hybrid nanofluid also serves as a thermal barrier and decreases the amount of heat transmitted to the cutting device, workpiece, and chip [79]. The reduced heat influences the cutting tool's material expansion, so the cutting edge's hardness is maintained for the longer cutting length. Besides, the nanocellulose containing composite nanofluid forms the impermanent interfacial layer on the cutting tool and decreases the cutting tool's wear.

Analysis comparison of tool failure between MWF and hybrid nanocoolant

Figure 19 shows that the tool life using hybrid nanofluid has shown a better result than using water coolant for every single parameter using the MQL system. The comparison graph shows that at machining parameter No. 7, hybrid nanofluid has significantly improved the cutting tool's life. MQL composite nanofluid takes 678 seconds to reach its wear criterion at 0.3mm. Meanwhile, MWF took 452 seconds to get the same wear criterion. The study by Uysal, Demiren [80] found that the MQL method can decrease the wear of the tool because engraved cutting fluid could reach the interface between the cutting tool and the workpiece. Also, the MQL flow rate has a positive impact on tool wear. So, an increase in the engraved cutting fluid amount can decrease the tool wear.
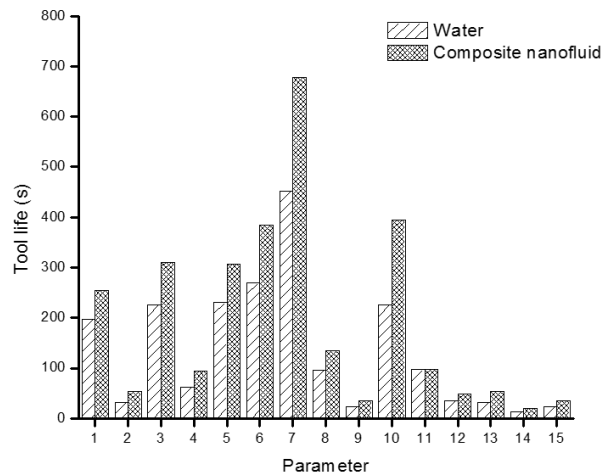
Figure 19. Comparison of machining tool life using MWF and composite or hybrid nanocoolant.

CONCLUSION

In this study, a new class coolant of hybrid nanocoolant has been formulated to enhance the machining behaviour. A linear mathematical model was developed to predict turning parameters for cylindrical mild steel, using WC-Co uncoated carbide tool on two different machining experiments using two different coolants: MWF and hybrid nanofluid. The hybrid coolant's thermophysical property was measured, and the performance was analysed by turning cylindrical mild steel using two different coolants (MWF and hybrid nanocoolant) utilising the MQL technique. The predicted linear model is used to get the best selection of turning parameters to reduce surface roughness, tool wear reduction, and improved cutting tool life based on RSM. Experimental results are compared with predicted results and the summarised findings as below:

i. Surface roughness is significantly affected by the spindle's cutting speed, feed rate, and followed by cutting depth in both machining experiments using normal water coolant or hybrid nanofluid. Based on this experimental analysis, the surface roughness reduces when the feed rate decreases and the cutting speed increases.

ii. Based on the mathematical modelling developed using RSM, the cutting speed has the most significant effect on the surface roughness and tool wear, followed by the feed rate. It is seen the depth of cut does not significantly affect the tool wear and surface roughness.

iii. Based on the observation, flank wear is highest when turning the mild steel using MWF coolant. Besides, shorter tool life was obtained using the MWF coolant.

iv. Though, using the nanocoolant composite (nanocellulose + alumina), the total length of cut was found to increase during the turning operation of mild steel workpiece at similar. It shows that the predicted values satisfied the experimental findings with less than 10% of error.

v. The addition of the hybrid nanofluid has the lowest surface roughness and reduces the tool wear because it boosts the heat transfer rate and increases the thermal conductivity.

vi. The turning process using MQL hybrid nanofluid coolant has outperformed MQL MWF coolant in terms of surface roughness and tool life. The better surface roughness produced after using MQL hybrid nanofluid coolant is 1.026 μm while using MQL normal water coolant is 1.458 μm. Thus, the hybrid nanofluid has improved the surface roughness by 29.63 %. Significant enhancement was observed in the longer tool total length of cut (39%) by utilising the prepared hybrid nano lubricant compared to MWF. The maximum tool life produced for the turning process until the wear reaches the ISO 3685:1993 wear criterion is 0.3 mm and 678 seconds by using MQL hybrid nanofluid coolant while using MQL normal water coolant 452 seconds. There is also an improvement in the cutting tool lifespan, which has increased by about 33.33 % longer.

ACKNOWLEDGEMENT

REFERENCES

[1] H. El-Hofy, *Fundamentals of Machining Processes: Conventional and Nonconventional Processes*. Boca Raton: CRC press, 2018

[2] J. Chae, S. Park, and T. Freiheit, "Investigation of micro-cutting operations," *Int. J. Mach. Tools Manuf.*, vol. 46, no. 3-4, p. 313-332, 2006, doi: 10.1016/j.ijmachtools.2005.05.015.

[3] P. Sreejith, and B. Ngoi, "Dry machining: machining of the future," *J. Mater. Process. Technol.*, vol. 101, no. 1-3, p. 287-291, 2000, doi: 10.1016/S0924-0136(00)00445-3.

[4] S. Debnath, M.M. Reddy, and Q.S. Yi, "Environmental friendly cutting fluids and cooling techniques in machining: A review," *J. Clean. Prod.*, vol. 83, p. 33-47, 2014, doi: 10.1016/j.jclepro.2014.07.071.

[5]   Y. Yin, et al., "Lessons from seru production on manufacturing competitively in a high cost environment," *J. Oper. Manag.*, vol. 49, p. 67-76, 2017, doi: 10.1016/j.jom.2017.01.003.

[6]   A. Iles, and A.N. Martin, "Expanding bioplastics production: sustainable business innovation in the chemical industry," *J. Clean. Prod.*, vol. 45, p. 38-49, 2013, doi: 10.1016/j.jclepro.2012.05.008.

[7]   R. Ghoreishi, A.H. Roohi, and A.D. Ghadikolaei, "Analysis of the influence of cutting parameters on surface roughness and cutting forces in high speed face milling of Al/SiC MMC," *Mater. Res. Express*, vol. 5, no. 8, p. 086521, 2018, doi: 10.1088/2053-1591/aad164.

[8]   E. Benedicto et al., "The role of surfactant structure on the development of a sustainable and effective cutting fluid for machining titanium alloys," *Metals*, vol. 10, no. 10, p. 1388, 2020, doi: 10.3390/met10101388.

[9]   M.M. Khan, M. Mithu, and NR. Dhar, "Effects of minimum quantity lubrication on turning AISI 9310 alloy steel using vegetable oil-based cutting fluid," *J. Mater. Process. Technol.*, vol. 209, no. 15-16, p. 5573-5583, 2009, doi: 10.1016/j.jmatprotec.2009.05.014.

[10]   N. Dhar, M. Ahmed, and S. Islam, "An experimental investigation on effect of minimum quantity lubrication in machining AISI 1040 steel," *Int. J. Mach. Tools Manuf.*, vol. 47, no. 5, p. 748-753, 2007, doi: 10.1016/j.ijmachtools.2006.09.017.

[11]   MNF Abd Malek, et al., "Ultrasonication: A process intensification tool for methyl ester synthesis: A mini review," *Biomass Convers. Biorefin.*, p. 1-11, 2020, doi: 10.1007/s13399-020-01100-6.

[12]   H.-J. Kim et al., "Nano-lubrication: A review," *Int. J. Precis. Eng. Manuf.*, vol. 17, no. 6, p. 829-841, 2016.

[13]   M. Emami, et al., "Investigating the minimum quantity lubrication in grinding of Al2O3 engineering ceramic," *J. Clean. Prod.*, vol. 66, 632-643, 2014,doi: 10.1016/j.jclepro.2013.11.018.

[14]   M.K. Sinha, et al., "An alternate method for optimisation of minimum quantity lubrication parameters in surface grinding," *Int. J. Mach. Mach. Mater.*, vol. 18, no. 5-6, p. 586-605, 2016,doi: 10.1504/IJMMM.2016.078983.

[15]   S.A. Lawal, et al., "Vegetable-oil based metalworking fluids research developments for machining processes: survey, applications and challenges," *Manuf. Rev*, vol. 1, p. 22, 2014,doi: 10.1051/mfreview/2014021.

[16]   M. Jamil et al., "Sustainable milling of Ti–6Al–4V: A trade-off between energy efficiency, carbon emissions and machining characteristics under MQL and cryogenic environment," *J. Clean. Prod.*, vol. 281, p. 125374, 2020, doi: 10.1016/j.jclepro.2020.125374.

[17]   P. Bhuyar et al., "Synthesis of silver nanoparticles using marine macroalgae Padina sp. and its antibacterial activity towards pathogenic bacteria," *Beni Suef Univ. J. Basic Appl. Sci.*, vol. 9, no. 1, p. 1-15, 2020, doi: 10.1186/s43088-019-0031-y.

[18]   S.A. Shaw, "A review of nanofluids synthesis for oil and gas applications," in 2020 IEEE 15th International Conference on Nano/Micro Engineered and Molecular System (NEMS), Virtual Conference, 2020.

[19]   D.D. Kumar, and A.V. Arasu, "A comprehensive review of preparation, characterisation, properties and stability of hybrid nanofluids," *Renew. Sust. Energ. Rev.*, vol. 81: p. 1669-1689, 2018, doi: 10.1016/j.rser.2017.05.257.

[20]   N.A.C Sidik et al., "Recent progress on the application of nanofluids in minimum quantity lubrication machining: A review," *Int. J. Heat Mass Transf.*, vol. 108, p. 79-89, 2017, doi: 10.1016/j.ijheatmasstransfer.2016.11.105.

[21]   K. Suganthi, and K. Rajan, Metal oxide nanofluids: Review of formulation, thermo-physical properties, mechanisms, and heat transfer performance. *Renew. Sust. Energ. Rev.*, vol. 76, p. 226-255, 2017, doi: 10.1016/j.rser.2017.03.043.

[22]   B. Wei et al., "Thermo-physical property evaluation of diathermic oil based hybrid nanofluids for heat transfer applications," *Int. J. Heat Mass Transf.*, vol. 107, p. 281-287, 2017,doi: 10.1016/j.ijheatmasstransfer.2016.11.044.

[23]   Y. Wang et al., "Processing characteristics of vegetable oil-based nanofluid MQL for grinding different workpiece materials," *Int. J. Precis. Eng. Manuf. – Gr. Tech.,* vol. 5, no. 2, p. 327-339, 2018,doi: 10.1007/s40684-018-0035-4.

[24]   C. Mao, et al., "The influence of spraying parameters on grinding performance for nanofluid minimum quantity lubrication," *Int. J. Adv. Manuf. Syst.*, vol. 64, p. 1791-1799, 2013, doi: 10.1007/s00170-012-4143-y.

[25]   C. Mao et al., "The tribological properties of nanofluid used in minimum quantity lubrication grinding," *Int. J. Adv. Manuf. Technol.*, vol. 71, no. 5, p. 1221-1228, 2014,doi: 10.1007/s00170-013-5576-7.

[26]   D. Setti et al., "Performance evaluation of Ti–6Al–4V grinding using chip formation and coefficient of friction under the influence of nanofluids," *Int. J. Mach. Tools Manuf.*, vol. 88, p. 237-248, 2015, doi: 10.1016/j.ijmachtools.2014.10.005.

[27]   A.K. Sharma et al., "Characterisation and experimental investigation of Al2O3 nanoparticle based cutting fluid in turning of AISI 1040 steel under minimum quantity lubrication (MQL)," *Mater. Today: Proc.*, vol. 3, no. 6, p. 1899-1906, 2016, doi: 10.1016/j.matpr.2016.04.090.

[28]   V. Gaitonde, S. Karnik, and J.P. Davim, "Selection of optimal MQL and cutting conditions for enhancing machinability in turning of brass," *J. Mater. Process. Technol.*, vol. 204, no. 1-3, p. 459-464, 2008,doi: 10.1016/j.jmatprotec.2007.11.193.

[29]   U. Nithiyanantham et al., "Shape effect of Al2O3 nanoparticles on the thermophysical properties and viscosity of molten salt nanofluids for TES application at CSP plants," *Appl. Therm. Eng.*, vol. 169, p. 114942, 2020, doi: 10.1016/j.applthermaleng.2020.114942.

[30]   D. Trache et al., "Nanocellulose: from fundamentals to advanced applications," *Front. Chem.*, vol. 8, 2020, doi: 10.3389/fchem.2020.00392.

[31]   L. Samylingam et al., "Thermal analysis of cellulose nanocrystal-ethylene glycol nanofluid coolant," *Int. J. Heat Mass Transf.*, vol. 127, p. 173-181, 2018, doi: 10.1016/j.ijheatmasstransfer.2018.07.080.

[32]   J. Buongiorno et al., "A benchmark study on the thermal conductivity of nanofluids," *Int. J. Appl. Phys.*, vol. 106, no. 9, p. 094312, 2009, doi: 10.1063/1.3245330.

[33]   M. Prakash et al., "Effect of machining configuration on the corrosion of mild steel," *J. Mater. Process. Technol.*, vol. 219, p. 70-83, 2015, doi: 10.1016/j.jmatprotec.2014.11.044.

[34]   S. Zaefferer, S. Wright, and D. Raabe, "Three-dimensional orientation microscopy in a focused ion beam–scanning electron microscope: A new dimension of microstructure characterisation," *Metall. Mater. Trans. A*, vol. 39, no. 2, p. 374-389, 2008,doi: 10.1007/s11661-007-9418-9.

[35]   M. Hadadian et al., "Nanofluids for heat transfer enhancement–a review," *Phys. Chem. Res.*, vol. 1, no. 1, p. 1-33, 2013,doi: 10.22036/pcr.2013.2791.

[36]   K. Ramachandran et al., "Thermophysical properties measurement of nano cellulose in ethylene glycol/water," *Appl. Therm. Eng.*, vol. 123, p. 1158-1165, 2017, doi: 10.1016/j.applthermaleng.2017.05.067.

[37]   P. Maheshwary, and K. Nemade, "Enhancement in heat transfer performance of ZrO2/H2O nanofluid via ultrasonication time," *International Journal on Recent and Innovation Trends in Computing and Communication (IJRITCC)*, vol. 3, no. 2, p. 35-37, 2015,.

[38]   LS Sundar, M.K. Singh, and A.C. Sousa, "Thermal conductivity of ethylene glycol and water mixture based Fe₃O₄ nanofluid," *Int. Commun. Heat Mass Transf.*, vol. 49, p. 17-24, 2013,doi: 10.1016/j.icheatmasstransfer.2013.08.026.

[39]   M. Sarafraz, and F. Hormozi, "Scale formation and subcooled flow boiling heat transfer of CuO–water nanofluid inside the vertical annulus," *Exp. Therm. Fluid Sci.*, vol. 52, p. 205-214, 2014,doi: 10.1016/j.expthermflusci.2013.09.012.

[40]   Y. Sheng et al., "Aggregation behavior and foam properties of the mixture of hydrocarbon and fluorocarbon surfactants with addition of nanoparticles," *J. Mol. Liq.*, p. 115070, 2020, doi: 10.1016/j.molliq.2020.115070.

[41]   S. Habibzadeh et al., "Stability and thermal conductivity of nanofluids of tin dioxide synthesised via microwave-induced combustion route," *Chem. Eng. Sci.*, vol. 156, no. 2, p. 471-478, 2010,doi: 10.1016/j.cej.2009.11.007.

[42]   Z. Chen et al., "The impact of sonication and stirring durations on the thermal conductivity of alumina-liquid paraffin nanofluid: an experimental assessment. *Powder Technol.*, vol. 360, p. 1134-1142, 2020, doi: 10.1016/j.powtec.2019.11.036.

[43]   I. Wole-Osho et al., An experimental investigation into the effect of particle mixture ratio on specific heat capacity and dynamic viscosity of Al2O3-ZnO hybrid nanofluids. *Powder Technol.*, vol. 363, p. 699-716, 2020, doi: 10.1016/j.powtec.2020.01.015.

[44]   S.N.A. Shah, S. Shahabuddin, and MFM Sabri, "Evaluation of thermal conductivity, stability and viscosity of two dimensional hexagonal boron nitride nanofluids," *Int. J. Adv. Sci. Technol.*, vol. 29, no. 1, p. 304-317, 2020,.

[45]   F. Hatami, and F. Okhovati, "Analysis of turbulent flow of nanofluids in a pipe," *Eur. Online J. Nat. Soc. Sci.*, vol. 3, no. 3 (s), p. 72-85, 2014.

[46]   A. Meriläinen et al., "Influence of particle size and shape on turbulent heat transfer characteristics and pressure losses in water-based nanofluids," *Int. J. Heat Mass Transf.*, vol. 61, p. 439-448, 2013,doi: 10.1016/j.ijheatmasstransfer.2013.02.032.

[47]   H. Chiam et al., "Thermal conductivity and viscosity of Al2O3 nanofluids for different based ratio of water and ethylene glycol mixture," *Exp. Therm. Fluid Sci.*, vol. 81, p. 420-429, 2017, doi: 10.1016/j.expthermflusci.2016.09.013.

[48]   A. Acevedo-Fani et al., "Edible films from essential-oil-loaded nanoemulsions: Physicochemical characterisation and antimicrobial properties," *Food Hydrocoll.*, vol. 47, p. 168-177, 2015, doi: 10.1016/j.foodhyd.2015.01.032.

[49]   R.S. Vajjha, and DK. Das, "Experimental determination of thermal conductivity of three nanofluids and development of new correlations," *Int. J. Heat Mass Transf.*, vol. 52, no. 21-22, p. 4675-4682, 2009,doi: 0.1016/j.ijheatmasstransfer.2009.06.027.

[50]   F. Hirosawa, T. Iwasaki, and M. Iwata, "Kinetic analysis of mechanochemical reaction between zinc oxide and gamma ferric oxide based on the impact energy and collision frequency of particles," *Powder Technol.*, vol. 352, p. 360-368, 2019,doi: 10.1016/j.powtec.2019.04.050.

[51]   Y. Li et al., "Effects of sonication duration and nanoparticles concentration on thermal conductivity of silica-ethylene glycol nanofluid under different temperatures: An experimental study," *Powder Technol.*, vol. 367, p. 464-473, 2020, doi: 10.1016/j.powtec.2020.03.058.

[52]   NK. Sahu, A.B. Andhare, and R.A. Raju, "Evaluation of performance of nanofluid using multiwalled carbon nanotubes for machining of Ti–6AL–4V," *Mach. Sci. Technol.*, vol. 22, no. 3, p. 476-492, 2018, doi: 10.1080/10910344.2017.1365898.

[53]   A.A. Hamid, and O.O. Aiyelaagbe, "Pharmacological investigation of Asystasia calyciana for its antibacterial and antifungal properties," *Int. J. Chem. Biochem. Sci.*, vol. 1, p. 99-104, 2012,.

[54]   M. Nabi et al., "Detailed simulation of morphodynamics: 3. Ripples and dunes," *Water Resour. Res.*, vol. 49, no. 9, p. 5930-5943, 2013, doi: 10.1002/wrcr.20457.

[55]   M. Farbod, and A. Ahangarpour, "Improved thermal conductivity of Ag decorated carbon nanotubes water based nanofluids," Physics Letters A, vol. 380, no. 48, p. 4044-4048, 2016, doi: 10.1016/j.physleta.2016.10.014.

[56]   M. Esfahani et al., "Electrodeposition of nanocrystalline zinc from sulfate and sulfate-gluconate electrolytes in the presence of additives," *J. Electrochem. Soc.*, vol. 163, no. 9, p. D476-484, 2016, doi: 10.1149/2.0471609jes.

[57]   P.S. Kulkarni, J.G. Crespo, and C.A. Afonso, "Dioxins sources and current remediation technologies—a review," *Environ. Int.*, vol. 34, no. 1, p. 139-153, 2008, doi: 10.1016/j.envint.2007.07.009.

[58]   R.S. Vajjha, D.K. Das, and P.K. Namburu, "Numerical study of fluid dynamic and heat transfer performance of Al2O3 and CuO nanofluids in the flat tubes of a radiator," *Int. J. Heat Fluid Flow*, vol. 31, no. 4, p. 613-621, 2010, doi: 10.1016/j.ijheatfluidflow.2010.02.016.

[59]   M. Kole, and T. Dey, "Thermal conductivity and viscosity of Al2O3 nanofluid based on car engine coolant," *J. Phys. D: Appl. Phys.*, vol. 43, no. 31, p. 315501, 2010, doi: 10.1088/0022-3727/43/31/315501.

[60]   P.K. Namburu et al., "Viscosity of copper oxide nanoparticles dispersed in ethylene glycol and water mixture," *Exp. Therm. Fluid Sci.*, vol. 32, no. 2, p. 397-402, 2007, doi: 10.1016/j.expthermflusci.2007.05.001.

[61]   L. Fedele, L. Colla, and S. Bobbo, "Viscosity and thermal conductivity measurements of water-based nanofluids containing titanium oxide nanoparticles," *Int. J. Refrig.*, vol. 35, no. 5, p. 1359-1366, 2012, doi: 10.1016/j.ijrefrig.2012.03.012.

[62]   X. Li et al., "Nonthermally dominated electron acceleration during magnetic reconnection in a low-β plasma," *Astrophys. J. Lett.*, vol. 811, no. 2, p. L24, 2015, doi: 10.1088/2041-8205/811/2/L24.

[63]   A. Asadi and I.M. Alarifi, "Effects of ultrasonication time on stability, dynamic viscosity, and pumping power management of MWCNT-water nanofluid: an experimental study," *Sci. Rep.*, vol. 10, no. 1, p. 1-10, 2020, doi: 10.1038/s41598-020-71978-9.

[64]   Y. Hua, and Z. Liu, "Effects of cutting parameters and tool nose radius on surface roughness and work hardening during dry turning Inconel 718," *Int. J. Adv. Manuf. Technol.*, vol. 96, no. 5-8, p. 2421-2430, 2018, doi: 10.1007/s00170-018-1721-7.

[65]   A.T. Abbas et al., "Towards optimisation of surface roughness and productivity aspects during high-speed machining of Ti–6Al–4V," *Materials*, vol. 12, no. 22, p. 3749, 2019, doi: 10.3390/ma12223749.

[66]   S. Kumar, D. Singh, and NS. Kalsi, "Analysis of Surface Roughness during Machining of Hardened AISI 4340 Steel using Minimum Quantity lubrication," *Mater. Today: Proc.*, vol. 4, no. 2, Part A, p. 3627-3635, 2017, doi: 10.1016/j.matpr.2017.02.255.

[67]   W. Khaliq et al., "Tool wear, surface quality, and residual stresses analysis of micro-machined additive manufactured Ti–6Al–4V under dry and MQL conditions," *Tribol. Int.*, p. 106408, 2020, doi: 10.1016/j.triboint.2020.106408.

[68]   O. Özbek, and H. Saruhan, "The effect of vibration and cutting zone temperature on surface roughness and tool wear in eco-friendly MQL turning of AISI D2," *J. Mater. Res. Technol.*, 2020, doi: 10.1016/j.jmrt.2020.01.010.

[69]   M. Kuntoğlu et al., "Optimisation and analysis of surface roughness, flank wear and 5 different sensorial data via tool condition monitoring system in turning of aisi 5140," *Sensors*, vol. 20, no. 16, p. 4377, 2020, doi: 10.3390/s20164377.

[70]   E.A. Rahim, A.S.A. Sani, and N. Talib, "Tribological interaction of bio-based metalworking fluids in machining process," *Lubrication Tribology, Lubricants and Additives*, p. 45, 2018, doi: 10.5772/intechopen.72511.

[71]   S. Debnath, M.M. Reddy, and Q.S. Yi, "Influence of cutting fluid conditions and cutting parameters on surface roughness and tool wear in turning process using Taguchi method," *Measurement*, vol. 78, p. 111-119, 2016, doi: 10.1016/j.measurement.2015.09.011.

[72]   Ç.V. Yıldırım et al., "The effect of addition of hBN nanoparticles to nanofluid-MQL on tool wear patterns, tool life, roughness and temperature in turning of Ni-based Inconel 625," *Tribol. Int.*, vol. 134, p. 443-456, 2019, doi: 10.1016/j.triboint.2019.02.027.

[73]   A. Altin, M. Nalbant, and A. Taskesen, "The effects of cutting speed on tool wear and tool life when machining Inconel 718 with ceramic tools," *Mater. Des.*, vol. 28, no. 9, p. 2518-2522, 2007,doi: 10.1016/j.matdes.2006.09.004.

[74]   S. Koseki et al., "Wear mechanisms of PVD-coated cutting tools during continuous turning of Ti-6Al-4V alloy," *Precision Engineering*, vol. 47, p. 434-444, 2017,doi: 10.1016/j.precisioneng.2016.09.018.

[75]   V. Vasu and G. Pradeep Kumar Reddy, "Effect of minimum quantity lubrication with Al2O3 nanoparticles on surface roughness, tool wear and temperature dissipation in machining Inconel 600 alloy," *Proceedings of the Institution of Mechanical Engineers, Part N: Journal of Nanoengineering and Nanosystems*, vol. 225, no. 1, p. 3-16, 2011,doi: 10.1177/1740349911427520.

[76]   A. Khan and K. Maity, "Influence of cutting speed and cooling method on the machinability of commercially pure titanium (CP-Ti) grade II," *J. Manuf. Process.*, vol. 31, p. 650-661, 2018,doi: 10.1016/j.jmapro.2017.12.021.

[77]   M. Mia et al., "Multi-objective optimisation of chip-tool interaction parameters using Grey-Taguchi method in MQL-assisted turning," *Measurement*, vol. 129, p. 156-166, 2018,doi: 10.1016/j.measurement.2018.07.014.

[78]   A. Moris Devotta et al., "Predicting Continuous Chip to Segmented Chip Transition in Orthogonal Cutting of C45E Steel through Damage Modeling," *Metals*, vol. 10, no. 4, p. 519, 2020,doi: 10.3390/met10040519.

[79]   K. Kadirgama, "Nanofluid as an alternative coolant in machining: A review," *J. Adv. Res. Fluid Mech. Therm. Sci.*, vol. 69, no. 1, p. 163-173, 2020, doi: 10.37934/arfmts.69.1.163173.

[80]   A. Uysal, F. Demiren, and E. Altan, "Applying minimum quantity lubrication (MQL) method on milling of martensitic stainless steel by using nano MoS2 reinforced vegetable cutting fluid," *Procedia Soc. Behav. Sci.*, vol. 195, p. 2742-2747, 2015, doi: 10.1016/j.sbspro.2015.06.384.